Received: 19 August 2025 | Accepted: 10 August 2026

DOI: 10.1111/1365-2435.70439

Functional Ecology

RESEARCH ARTICLE

Stem water content predicts drought-induced mortality in tropical semiarid species

Lussarina Oliveira Lima[1] | Angela Lucena Nascimento Jesus[1] | Vivian Barros Talmag[2] | Rafael Silva Oliveira[3] | Francisca Soares de Araújo[1,2] | Arlete Aparecida Soares[1,2] | Cleiton Breder Eller[1,2]

[1]Ecology and Natural Resources Post-Graduate Program, Department of Biology, Federal University of Ceará, Fortaleza, Ceará, Brazil

[2]Department of Biology, Federal University of Ceará, Fortaleza, Ceará, Brazil

[3]Department of Plant Biology, University of Campinas, Campinas, São Paulo, Brazil

Correspondence
Cleiton Breder Eller
Email: ellercb@ufc.br

Funding information
Instituto Serrapilheira, Grant/Award Number: AJC-0222-00006.01.00/24; Coordenação de Aperfeiçoamento de Pessoal de Nível Superior; Fundação Cearense de Apoio ao Desenvolvimento Científico e Tecnológico - FUNCAP; National Council for Scientific and Technological Development, Grant/Award Number: 408930/2024-1; São Paulo Research Foundation, Grant/Award Number: 2025/28192-8

Handling Editor: Benjamin Hafner

Abstract

1. Hydraulic Failure is one of the primary mechanisms underlying plant mortality during drought. Hydraulic failure occurs when the plant's xylem, under water stress, crosses a critical percentage of loss of xylem hydraulic conductivity (PLC) threshold, which causes the plant's tissues to desiccate and die. The PLC threshold that triggers mortality varies between different taxa and functional types and remains largely undefined for plants from tropical seasonally dry formations (TSDF)—biodiverse and drought-prone ecosystems.
2. Recent studies have proposed that stem Relative Water Content (RWC) thresholds might be more useful predictors of drought-induced mortality due to their direct link with cell mortality. This implies that a different set of functional traits, which control plant tolerance to dehydration, also plays an important role in plant drought-induced mortality.
3. This study investigated whether PLC or RWC thresholds predict drought-induced mortality more accurately for two TSDF species with contrasting leaf phenology. We conducted a drought experiment with two TSDF species, the drought-deciduous *Cordia oncocalyx* and the evergreen *Cynophalla flexuosa*.
4. Our results reveal that both species can survive PLC >99%, suggesting that extreme embolism alone does not always lead to mortality. However, the evergreen species succumbed when its stem Relative Water Content (RWC) declined close to 37%. The deciduous species withstood a PLC over 99% for more than 20 days and recovered rapidly after rehydration, likely due to its higher stem water storage capacity and quick leaf shedding.
5. Our findings show that maintaining a high RWC, rather than only avoiding hydraulic failure, is key to the survival of TSDF species during drought. The deciduous species' leaf shedding and higher stem water content allowed it to sustain its RWC for longer during drought, making it less vulnerable to drought-induced

This is an open access article under the terms of the Creative Commons Attribution License, which permits use, distribution and reproduction in any medium, provided the original work is properly cited.
© 2026 The Author(s). *Functional Ecology* published by John Wiley & Sons Ltd on behalf of British Ecological Society.

mortality. The RWC thresholds identified in this study provide a key parameter to improve model projections of TSDF vegetation mortality during future droughts.

KEYWORDS
Caatinga, drought, hydraulic failure, leaf phenology, plant mortality

1 | INTRODUCTION

Widespread tree mortality events have become more common worldwide, threatening the functioning and distribution of forests (Allen et al., 2010; Hammond et al., 2022). One of the main physiological mechanisms underlying plant mortality during drought is the collapse of its hydraulic system, commonly referred to as Hydraulic Failure (Choat et al., 2018; McDowell et al., 2008, 2022). Hydraulic failure occurs when a large fraction of the plant's xylem is embolised, so that the xylem can no longer supply the water required to maintain plant tissues alive (Adams et al., 2017; Choat et al., 2018; McDowell et al., 2008, 2022). Mortality induced by hydraulic failure is generally thought to be irreversibly triggered when plants lose a certain percentage of xylem hydraulic conductance (Brodribb & Cochard, 2009; Choat et al., 2018; Hammond et al., 2019). Initially, it has been suggested that a Percentage Loss of xylem hydraulic Conductivity (PLC) of around 50% and 80% could define a 'point of no return' for mortality in gymnosperms and angiosperms, respectively (Brodribb & Cochard, 2009; Tyree et al., 2003; Urli et al., 2013). However, current research shows that the critical PLC that induces mortality varies significantly between species, with some surviving PLC higher than 90% (Adams et al., 2017; Hammond et al., 2019; Mantova et al., 2021). Adams et al. (2017) suggest this variation can be attributed to the difference in how species recover from embolism. This variation limits the use of PLC thresholds in vegetation models to predict shifts in vegetation caused by drought-induced mortality (McDowell et al., 2013; Trugman et al., 2021; Venturas et al., 2021).

More recently, plant water pools were proposed as more reliable predictors of plant mortality, as they reflect whole-plant water balance and have a strong mechanistic link with cell and tissue mortality (Martinez-Vilalta et al., 2019). This perspective suggests that hydraulic failure alone might not necessarily lead to plant mortality if it is not associated with tissue desiccation. Some plants, especially from more arid environments, have high water storage capacity (Lima et al., 2012; Wright et al., 2021) and other strategies that can delay tissue desiccation (Blackman et al., 2016). Consequently, their xylem might embolise substantially, but their tissues can remain hydrated and with the potential to recover, through the production of new xylem vessels (Brodribb & Cochard, 2009), or potentially other active mechanisms (Nardini et al., 2011; Love & Sperry, 2018; but see Choat et al., 2019). Despite the solid theoretical basis linking water content to cell and tissue mortality, there is scarce empirical evidence that tissue water content is indeed a better predictor of whole-plant mortality than PLC (Mantova et al., 2021).

Given the diversity of processes and thresholds involved in plant drought-induced mortality, predicting large-scale vegetation mortality requires knowledge of how different plant functional types succumb during drought. We are not aware of any studies that establish drought-induced mortality thresholds for Tropical Seasonally Dry Forests (TSDF) species, which limits our ability to predict how this vegetation type responds to more extreme drought. The lack of information on mortality thresholds for this type of tropical vegetation is a critical knowledge gap, as TSDF are one of the most extensive types of tropical forests (Murphy & Lugo, 1986) and play important roles in biogeochemical cycles and climate regulation (Maass et al., 2005; Siyum, 2020). Moreover, many TSDF regions are projected to experience more arid conditions in the future (Marengo et al., 2017; Tomasella et al., 2025), making research on drought-tolerance thresholds in this biome particularly urgent.

Despite its importance, TSDF functioning remains understudied compared to more humid forests (Muenchow et al., 2018; Siyum, 2020). Plants in TSDF employ contrasting ecological strategies to cope with seasonal water deficits. Deciduous species shed their leaves during the dry season to limit transpiration and often exhibit higher water storage capacity and hydraulic conductivity. In contrast, evergreen and late-deciduous species retain their foliage and might rely on one or more drought-tolerance strategies, such as conservative stomatal regulation, high resistance to xylem embolism and access to deep soil water through extensive root systems (Lima et al., 2012; Lopes et al., 2022; Oliveira et al., 2021; Pereira et al., 2019; Tomlinson et al., 2013; Wright et al., 2021).

In this study, we investigate the drought-induced mortality thresholds of two tropical woody species with contrasting leaf phenologies: the drought-deciduous *Cordia oncocalyx* and the evergreen *Cynophalla flexuosa*. Both species are endemic to the TSDF from northeastern Brazil (Moro et al., 2016). We designed an experiment to establish whether PLC or stem Relative Water Content (RWC) thresholds are more useful predictors of plant mortality during drought and whether these thresholds vary depending on leaf phenology. Our first hypothesis is that RWC thresholds are better predictors of mortality during drought (Kursar et al., 2009; Mantova et al., 2021, 2023; Martinez-Vilalta et al., 2019). This hypothesis is based on the rationale that although hydraulic failure is a prerequisite for RWC decline, it does not necessarily lead to lethal tissue desiccation if the plant still has living cells that can reconstruct (or repair) its hydraulic system. Our second hypothesis is that drought-deciduous and evergreen species have different tolerance to desiccation after hydraulic failure due to their functional differences. As drought-deciduous species shed their leaves

quickly during drought and often present higher wood water content (Lima et al., 2012; Wright et al., 2021), we expect their tissues to desiccate more slowly during drought. In contrast, we expect the evergreen species to rely especially on stomatal regulation to avoid embolism and desiccation.

2 | MATERIALS AND METHODS

2.1 | Study species

The study was carried out in a greenhouse at the Federal University of Ceará (3°44′19″ S; 38°34′13″ W). We used saplings of the species *Cordia oncocalyx* Allemão, a model deciduous species and *Cynophalla flexuosa* (L.) J. Presl, as a model evergreen species. Both species can grow as trees or shrubs and are endemic to the Caatinga (Lima et al., 2018). The Caatinga is a semiarid morphoclimatic domain characterised by average temperatures between 25° and 30°C and annual rainfall between 500 and 750 mm, distributed over a short-wet season lasting 3 to 5 months (Sampaio, 1995).

The species used in this study are functionally distinct in several ways beyond their leaf phenology. The deciduous species exhibits lower wood density, higher stem water content and xylem more vulnerable to embolism than that of the evergreen species (Table 1). In terms of leaf structure, some deciduous species of the Caatinga have a higher stomatal density, a higher leaf area and their leaf surfaces are covered with trichomes (Accioly et al., 2024; Araújo et al., 2024). Meanwhile, the evergreen *C. flexuosa* leaves are characterised by a thick cuticle and stomata protected by a prominent grooved epicuticular border (Holanda et al., 2019; Lopes et al., 2022; Pereira et al., 2019).

Seedlings of both species were collected in a Caatinga site located at the municipality of Pentecoste (3°49′02″ S; 39°20′16″ W). The seedlings were collected by manual excavation, keeping the soil around the roots intact to minimise damage. They were transplanted into 8-L pots filled with a substrate made up of a 2:2:1 mixture of sand, soil from the site where the plants were collected and organic-rich commercial substrate. They were then left to acclimatise for 6 months in the greenhouse.

2.2 | Experimental design

We used a total of 34 saplings of *C. oncocalyx* (11 of which were used for destructive RWC measurements) and 36 individuals of *C. flexuosa* for the drought experiments (10 of which were used for destructive RWC measurements). The *C. oncocalyx* at the beginning of the experiment had an average height of 49 ± 13.22 cm, while *C. flexuosa* individuals had an average height of 70.54 ± 13.22 cm. The water deficit during the experiment was imposed gradually; in the first week, the plants were watered with 200 mL of water every 2 days; in the second week, 100 mL every 2 days; in the third week, 50 mL every 2 days. After the fourth week, we stopped watering the plants altogether.

As the water content in the soil decreased, we removed between 2 and 3 plants from the drought treatment, one of which was destroyed to measure the RWC, and the others were subjected to a rehydration treatment to confirm whether the plant was dead or not. Plants in the rehydration treatment were watered twice a day to maintain their soil near field capacity. Individuals in the rehydration treatment were considered dead when they did not produce any new tissues after 2 months of rehydration. The drought treatment was maintained until the soil completely dried out (i.e. the soil water content stabilised close to zero). The duration of the drought treatment for *C. oncocalyx* was 37 days and for *C. flexuosa* it was 69 days. Environmental conditions during the experiment are given in Figure S1; and a graphical description of the experimental design and sampling for each measurement is given in Figure 1.

2.3 | Leaf gas-exchange measurements

Gas-exchange measurements were taken on two fully expanded leaves between the second and fourth nodes of all plants at the

TABLE 1 Parameters of the vulnerability curves of the xylem to embolism and Relative water Content (RWC) in the stem for deciduous species *Cordia oncocalyx* and the evergreen *Cynophalla flexuosa*.

Parameter	*C. oncocalyx*	*C. flexuosa*	Units	Description
a	1.53	0.82	MPa^{-1}	Shape of the embolism vulnerability curve
P_{50}	−1.47	−2.39	MPa	P_x when PLC = 50%
P_{88}	−2.80	−4.87	MPa	P_x when PLC = 88%
K_{max}	0.0163	0.0044	$kg\,m^{-1}\,s^{-1}\,MPa^{-1}$	Xylem maximum hydraulic conductivity
R_{max}	99.88	83.25	%	Maximum RWC
b	−0.27	−0.58	MPa^{-1}	Shape of the RWC curve
R_{50}	−6.13	−7.95	MPa	P_x when RWC = 50%
Q_{sat}	0.72 ± 0.10	0.66 ± 0.18	$g\,cm^{-3}$	Saturated stem water content normalised per sample
SWS	27.10 ± 12.39	10.50 ± 5.75	g	Stem water storage
W_d	0.55	0.57	$g\,cm^{-3}$	Wood density

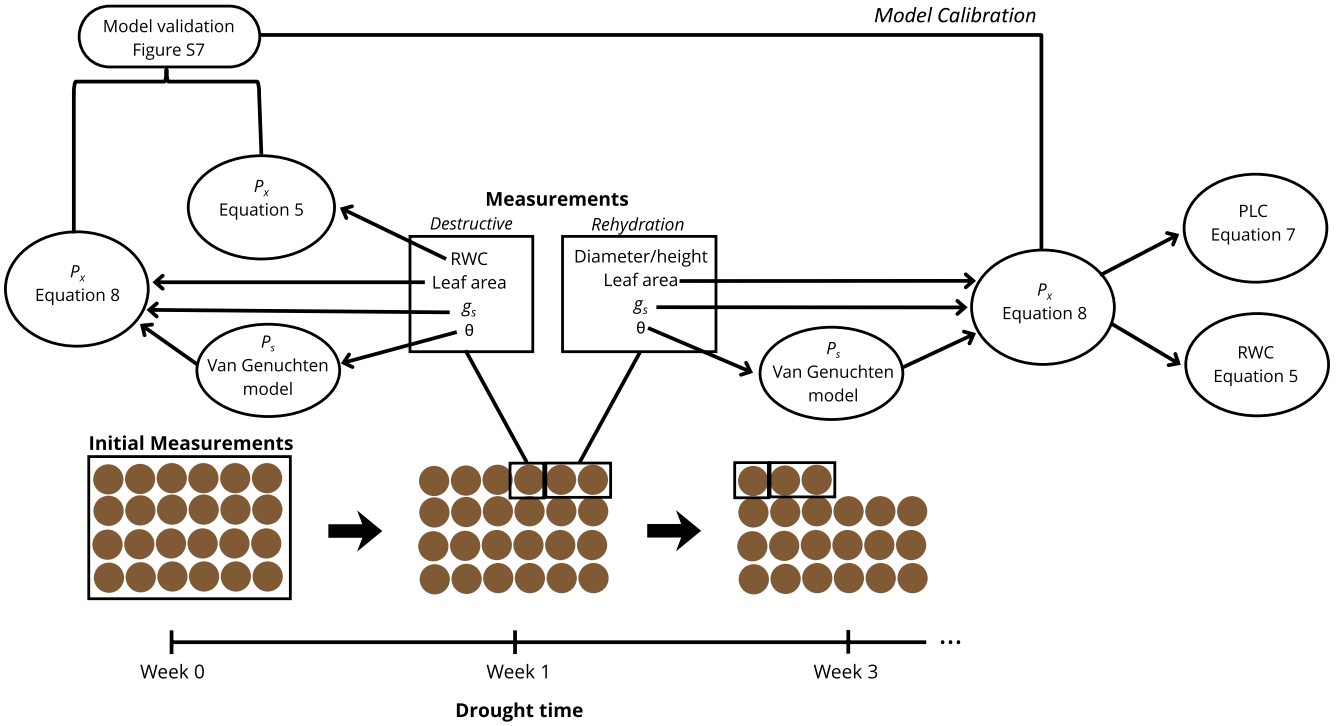


FIGURE 1 Diagram of the experimental design used during the drought experiment to assess species mortality of *Cordia oncocalyx* and *Cynophalla flexuosa*. Initial measurements were taken on all individuals, including growth measurements (height and diameter), leaf area, soil water content (θ) and gas-exchange measurements on 2–3 leaves. These measurements were also taken on individuals that were removed weekly. Individuals that underwent rehydration treatment were kept in moist soil for 3 months and monitored weekly (same initial measurements) to confirm mortality.

beginning of the experiment and when they were removed from the drought treatment. When the plant had senescent leaves, we also took a measurement on one of these leaves. The measurements were taken with a LI-6400XT gas-exchange analyser (Li-Cor BioSciences, Lincoln, NE, USA). The air temperature in the LI-6400XT measurement chamber was set to 25°C, relative humidity was maintained between 50% and 65%, the CO_2 concentration of the chamber was maintained at 400 ppm, the photosynthetically active photon flux density (PPFD) was set to 1800 μmol m^{-2} s^{-1}, and the air flow was set to 500 μmol s^{-1}.

2.4 | Leaf area and stem size measurements

Measurements of the plant total leaf area (L_a), stem diameter (D) and height (h) were taken on all individuals at the beginning of the experiment, when the individuals were removed from the drought treatment and at the end of the recovery treatment. The D was measured at the base and the top of the stem with a digital calliper with a resolution of 0.01 mm (MTX, Nicosia, Cyprus), and h was measured with a tape measure. The L_a was calculated as the sum of the total area of healthy ($L_{a,h}$) and senescent ($L_{a,s}$) leaves in the plant. All leaves on the plant had their length and width measured with a tape measure, which was then used to estimate the individual leaf area and subsequently L_a. See Supporting Information S1 for details.

2.5 | Soil water content and water potential

During the experiment, measurements of soil water content (SWC, %) in every pot were taken at intervals of 2 to 4 days with a portable soil moisture probe (Hydrosense II, Sensor Campbell, USA). We calibrated the SWC values measured with that sensor using gravimetric soil water content measurements (θ_g, g/g; Figure S2), see details of this calibration in Supporting Information S2. The θ_g was converted into volumetric soil water content (θ, cm^3/cm^3) using the bulk soil density and was used to calculate the soil water potential (P_s) using the Van Genuchten (1980) model (Figure S3). The parameters of the Van Genuchten model (Table S1) were estimated with a separate experiment described in Supporting Information S3.

2.6 | Stem water content

One of the individuals that was removed weekly from the drought treatment was used to measure the relative water content in the stem (RWC). This was a destructive measurement, as the plants did not have branches and the sample used for the RWC measurement was taken at the base of the stem (Figure S4). The RWC sample was *c*. 2 cm long and we measured its fresh weight (FW), turgid weight (TW) after 48 h emerged in distilled water and its dry mass (DW) by oven drying at 60°C for at least 72 h. We used an analytical balance

(BEL Engineering, MW723) for these measurements. We calculated the stem relative water content (RWC) as follows:

$$RWC = \frac{FW - DW}{TW - DW} 100 \quad (1)$$

We calculated the maximum mass of water stored per stem volume (Q_{sat}) as follows:

$$Q_{sat} = \frac{TW - DW}{V_s} \quad (2)$$

where V_s is the volume of the sample, which was measured with the water displacement method. From Q_{sat} we calculated the total maximum stem water storage (SWS) assuming a homogeneous water storage in the stem:

$$SWS = Q_{sat} V_p \quad (3)$$

As the saplings used in the experiment had no branches, we assumed that the stem volume (V_p) of the species could be approximated as a truncated cone, thus:

$$V_p = \pi \frac{h}{3} R^2 + R\, r^2 + r \quad (4)$$

where h is the stem height, and R and r are the radii of the stem base and top, respectively.

2.7 | Stem dehydration curve

We assessed the relationship between xylem water pressure (P_x) and stem Relative Water Content (RWC) to describe the process of stem dehydration in 12 individuals of the species *C. oncocalyx* and 10 of *C. flexuosa*. These individuals were not the same used for the drought experiment, but they were similarly sized plants that were collected at the same site and were maintained under identical conditions in the greenhouse. We started the curve with well-hydrated plants, covering four leaves of the plant with an opaque bag to balance the P_x. After 15 min, we measured the P_x using a Scholander chamber (Model 1515D, PMS Instrument Company, USA) on two leaves. We also conducted P_x measurements in leaves bagged for 1 h and found no significant effect of time on the measured P_x ($t = 1.44$; $p = 0.16$). This test was conducted to allow faster P_x measurements in the subsequent experiments described below.

We measured the RWC (Equation 1) of a stem segment close to the base of the plant, approximately 2 cm long immediately after each P_x measurement. We repeated this procedure until the P_x of the plants reached close to −9 MP. We then used a logistic function to describe the relationship between P_x and RWC:

$$RWC = \frac{R_{max}}{1 + \exp(b(P_x - R_{50}))} \quad (5)$$

where R_{max} is the RWC when $P_x = 0$, b controls the shape of the curve, and R_{50} is P_x when RWC = 50%. The curve obtained for both species is shown in Figure S5. Equation 5 was then used to estimate the P_x of the individuals during the drought experiment from their measured RWC (Figure 1).

2.8 | Xylem vulnerability to embolism

The vulnerability curve was constructed for each species using the bench drying technique of Sperry et al. (1988); see Supporting Information S4 for details (Figure S6). We used stem segments collected from 13 individuals of *C. oncocalyx* and 11 individuals of *C. flexuosa* to build the vulnerability curves. Similar to the stem dehydration curves, these individuals were not the same used for the drought experiment but had similar size and origin. The xylem hydraulic conductivity (K) was measured with a hydraulic apparatus based on Sperry et al. (1988). Before measuring K, the P_x was measured in two leaves previously bagged for 15 min using a Scholander-type pressure chamber (Model 1515D, PMS Instrument Company, USA). The Percentage Loss of xylem hydraulic Conductivity (PLC) was calculated as follows:

$$PLC = 100\left(1 - \frac{K}{K_{max}}\right) \quad (6)$$

The PLC data were used to build a vulnerability curve using the logistic equation proposed by Pammenter and Van Der Willigen (1998):

$$PLC = \frac{100}{1 + \exp\left(a\left(P_x - P_{50}\right)\right)} \quad (7)$$

where the parameters P_{50} and a are the value of P_x when PLC = 50% and the shape of the curve, respectively.

2.9 | Modelling xylem water pressure

In order to avoid interfering with the plant's recovery after drought, we used a model to estimate P_x, PLC and RWC at the end of the drought treatment (Figure 1). We calculated the PLC and RWC of the plants placed in the rehydration treatment after drought using Equations 5 and 7 and their P_x, which was modelled using the soil water potential data and a simple model derived from fundamental principles of plant hydraulic theory (Sperry & Love, 2015; Figure 1). The P_x was derived from the plant crown transpiration rate (E_c) and xylem hydraulic parameters with the following equation:

$$P_x = -\frac{\log\left(e^{-a\,P_{50}-\chi} + e^{-\chi - aP_{x,r}} - e^{-aP_{50}}\right)}{a} + \rho g h \quad (8a)$$

where ρ is water density and g is the acceleration due to Earth's gravity. The χ is a term proportional to E_c and a and inversely proportional to the whole-plant maximum xylem hydraulic conductance (k_{max}):

$$\chi = \frac{aE_c}{k_{max}} \quad (8b)$$

The derivation of Equation (8) is given in Supporting Information S5. The E_c used in Equation (8) was derived from the leaf gas-exchange measurements. We assumed the sapling canopy was relatively

homogeneous due to its small leaf area; therefore, E_c was scaled linearly to the sapling leaf area (L_a), taking only into consideration the differences in transpiration between healthy (E_h) and senescent (E_s) leaves:

$$E_c = E_h L_{a,h} + E_s L_{a,s} \quad (9)$$

We assumed that $E_c = 0$ when the plants were leafless, so we assumed $P_x \sim P_s$ as a first order approximation. Senescent leaves were visually classified as those exhibiting partial yellowing and/or browning of the leaf blade prior to abscission.

The P_x value calculated from Equation (8) and P_s were validated against the P_x calculated from the plant destructive RWC measurements during the experiment using Equation 5. The P_x from both approaches were strongly correlated ($R^2 = 0.78$ for *C. oncocalyx* and $R^2 = 0.99$ for *C. flexuosa*); however, the P_x values derived from P_s were systematically more negative at lower P_s (Figure S7) potentially indicating a soil–root decoupling (Delval et al., 2025). To account for this decoupling, we used the linear relationship presented in Figure S7 to correct the P_x estimates from the hydraulic model (Figure 1).

The k_{max} was calculated from the maximum xylem-specific hydraulic conductivity (K_{max}) estimated during the construction of the vulnerability curves, which was scaled to the whole plant using the plant dimensions:

$$k_{max} = K_{max} A_x / h \quad (10)$$

where A_x is the xylem area, assumed to be equal to the stem basal area.

2.10 | Replication statement

Analysis	Scale of inference	Scale at which the factor of interest is applied	Number of replicates at the appropriate scale
Comparing species	Species	Species	23[a]; 26[b]
Mortality predictor	Plant	Plant	49

[a] Cordia oncocalyx.

[b] Cynophalla flexuosa.

2.11 | Statistical analyses

2.11.1 | Mortality during drought

We used a bias-reduced logistic regression (Heinze & Schemper, 2002) to model the effect of PLC and RWC on the mortality data:

$$\log(\mu / (1 - \mu)) = \beta_0 + \beta_1 \text{PLC} + \beta_2 \text{RWC} \quad (11)$$

where μ is the expected value of the binary response variable (i.e. 1 for dead plants and 0 for surviving plants) and β_0, β_1 and β_2 are the empirical coefficients influencing the log-odds of mortality. Welch's *t*-tests were performed to evaluate the difference in RWC and PLC between dead and surviving individuals and differences between parameters of the RWC and PLC curves (Equations 5 and 7). The logistic regression fit was evaluated with likelihood ratio tests, McFadden pseudo-R^2 and Area Under the Curve (AUC) metrics (Hosmer Jr et al., 2013). We used a parametric Monte Carlo simulation based on the variance–covariance matrix of the model parameter estimates to propagate uncertainty in the probability of mortality.

2.11.2 | Leaf area, stomatal conductance and stem diameter responses to drought

The effect of P_x on the stomatal conductance (g_s) of healthy leaves of both species was modelled using an exponential function:

$$g_s = (a + \Delta a)(b + \Delta b)^{P_x} \quad (12)$$

where a is the stomatal conductance when $P_x = 0$ and $b = 1 + r$, where r is the compound rate of change of g_s per P_x increment. The Δa and Δb represent the species differences in each parameter. For this analysis (and all subsequent analyses), *C. flexuosa* is treated as the reference species; thus, Δa and Δb represent by how much a and b in *C. oncocalyx* differ from *C. flexuosa*.

We modelled the effect of P_x on the total plant leaf area (L_a) of both species using a Weibull function:

$$L_a = (a + \Delta a) e^{-\left((|P_x|/(b+\Delta b))^{(k+\Delta k)}\right)} \quad (13)$$

where a is L_a when $P_x = 0$, b is P_x when $L_a/a = 0.37$ and k controls the shape of the curve, with $k > 1$ resulting in a sigmoidal curve and $k \sim 1$ producing an exponential curve. The Δa, Δb and Δk are the species differences in each parameter.

The effect of P_x on stem diameter change during drought (D), computed as the difference between the stem diameter at the beginning and the end of the drought treatment, was evaluated with a linear model considering the effect of species on the D response to P_x:

$$D = (\beta_0 + \Delta\beta_0) + (\beta_1 + \Delta\beta_1) P_x \quad (14)$$

where β_0 and β_1 are the intercept and slope for *C. flexuosa*, and the $\Delta\beta_0$ and $\Delta\beta_1$ are the species differences in the model parameters.

2.11.3 | Leaf area and stem diameter recovery after drought

We calculated the recovery rate (R) for leaf area and stem diameter as follows:

$$R = \frac{(Y_{rec} - Y_{min})}{\Delta t} \quad (15)$$

where Y_{min} is the minimum value of leaf area and stem diameter observed during or after drought, Y_{rec} is the value after the recovery period, and Δt is the time in days between Y_{min} and Y_{rec}.

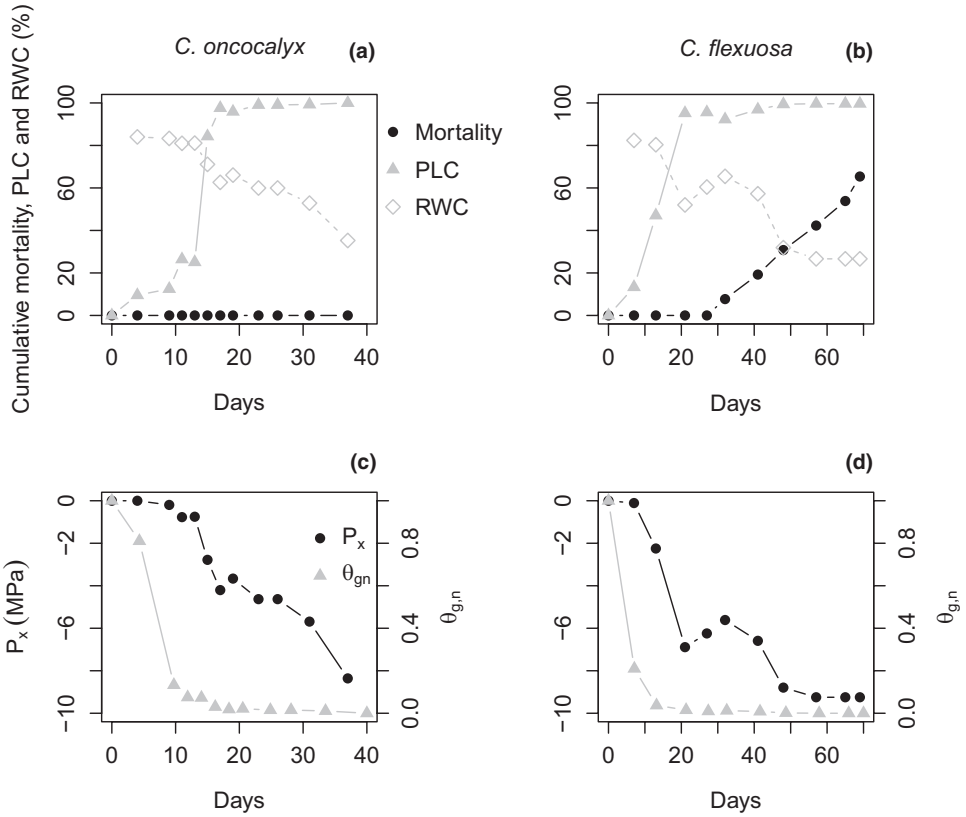


FIGURE 2 Cumulative mortality, Relative Water Content in stem (RWC) and Percentage Loss of xylem hydraulic Conductivity (PLC) during the drought experiment for the deciduous *Cordia oncocalyx* (a) and the evergreen *Cynophalla flexuosa* (b). The panels (c) and (d) are the modelled xylem water pressure (P_x) and the measured normalised soil moisture content ($\theta_{g,n}$) for *C. oncocalyx* and *C. flexuosa*, respectively.

We analysed the P_x effect on leaf area R using an exponential function identical to Equation 12. The stem diameter R was analysed with a linear model identical to Equation 14. For all statistical models used, assumptions were assessed through inspection of residuals and model fit (Zuur et al., 2010). The assumption of homoscedasticity of the residuals of the linear models was verified using the studentised Breusch-Pagan test (Breusch & Pagan, 1979; Koenker, 1981). All data analysis was conducted in *R* (R Core Team, 2024, v. 4.4.1) and the code is available on request.

3 | RESULTS

3.1 | Xylem hydraulics and stem water content

The xylem of the evergreen *C. flexuosa* was more resistant to embolism than the deciduous *C. oncocalyx* (Table 1; Figure S6). The P_{50} of *C. flexuosa* was 0.92 MPa more negative than *C. oncocalyx* ($t = 2.25$; $p = 0.02$), and its P_{88} was 2.07 MPa more negative ($t = -2.08$; $p = 0.03$). The xylem maximum hydraulic conductivity (K_{max}) was 3.6 times higher in *C. oncocalyx* than in *C. flexuosa* ($t = 2.63$; $p = 0.01$).

The stem relative water content (RWC) declined more gradually than PLC in response to more negative P_x (Figure 2a,b; Table 1). The deciduous species *C. oncocalyx* reaches lower RWC values at more negative P_x, due to the difference in the shape parameter between curves ($t = 2.76$; $p < 0.01$). However, the R_{50} parameter (P_x when RWC = 50%) did not differ between species, with *C. oncocalyx* exhibiting a value of −6.13 MPa and *C. flexuosa* of −7.95 MPa (Figure S5; Table 1). The Q_{sat} did not differ between the species, but the stem water storage (SWS) was significantly higher for *C. oncocalyx* ($t = 7.11$; $p < 0.01$; Table 1) due to its higher stem diameter.

3.2 | Soil water content and water potential

The normalised gravimetric soil water content ($\theta_{g'n}$) declined from 1 to very close to 0 during the drought treatment for both species (Figure 2c,d). The modelled xylem water pressure (P_x) obtained from Equation 5 followed the soil water dynamics. The P_x of plants during the drought experiment started at close to 0 MPa, reaching −8.36 MPa for *C. oncocalyx* and −9.25 MPa for *C. flexuosa* at the end of the experiment (Figure 2c,d).

3.3 | Mortality critical thresholds during drought

The PLC increased in both species during drought, with the PLC of the less embolism-resistant deciduous *C. oncocalyx* exceeding 99%

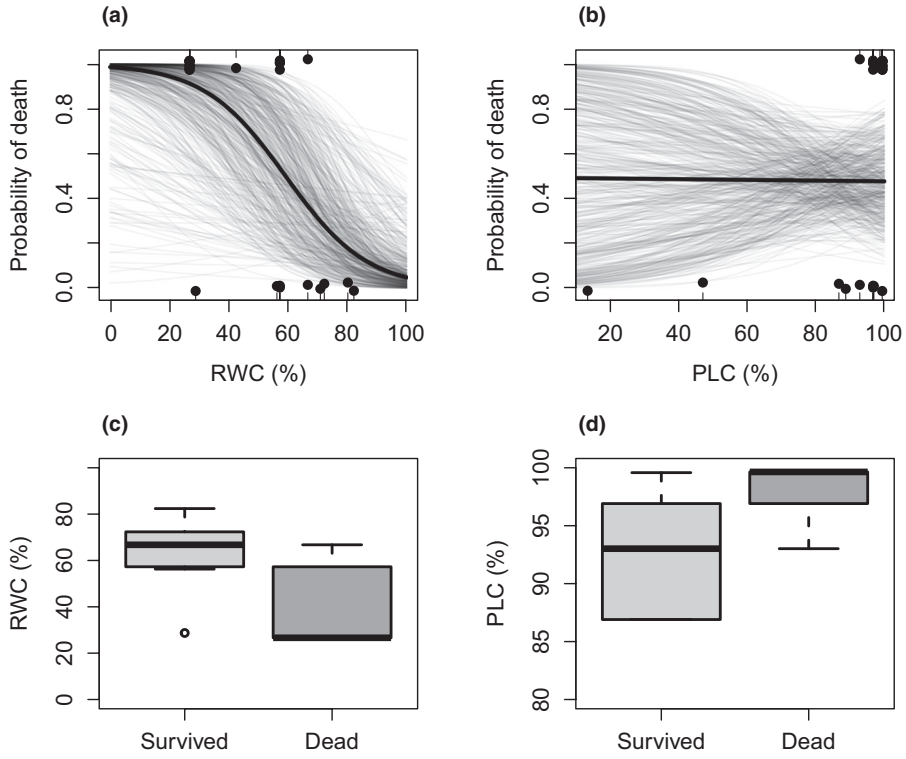


FIGURE 3 Probability of mortality as a function of the minimum Relative Water Content in the stem (RWC; a) and Percentage Loss of xylem hydraulic Conductivity (PLC; b) reached during the drought treatment for the evergreen *Cynophalla flexuosa*. The thick lines represent the conditional predictions of the logistic regression (Equation 11) with the variable not shown in each panel held constant at its mean value. The thin lines represent 500 curves generated by a parametric Monte Carlo simulation used to propagate prediction uncertainty (McFaddens $R^2 = 0.47$). Boxplots with the RWC (c) and PLC (d) of the individuals of *C. flexuosa* that survived and died during the drought.

TABLE 2 Estimated parameters of the logistic model (Equation 11) fitted to the effect of stem relative water content (RWC) and Percentage of Loss of hydraulic Conductivity (PLC) on probability of drought-induced mortality in species *Cynophalla flexuosa*.

Parameter	Estimate	SE	Lower CI 95%	Upper CI 95%	χ^2	*p* value
Intercept	4.32	3.97	−31	12.69	0.92	0.34
RWC	−0.072	0.03	−0.15	−0.01	5.58	0.02
PLC	−0.0006	0.03	−0.05	0.33	0.0005	0.98

after 15 days, while the more embolism-resistant *C. flexuosa* did so after 21 days (Figure 2a,b). The RWC in the deciduous species declined from 84% to 35.3%, while in the evergreen species it declined from 82.4% to 26.6% by the end of the experiment.

All the individuals of the deciduous *C. oncocalyx* survived over 20 days with a PLC >99% (Figure 2a). The evergreen *C. flexuosa* also could survive reaching a PLC >99%, but started succumbing after spending at least 11 days with a PLC >90% (Figure 2b). Consequently, all the individuals of *C. flexuosa* that died during the drought reached PLC >90% but not all individuals that reached PLC >90% died (Figure 3d). For example, one individual died after reaching a PLC of 93%, whereas others survived despite reaching PLC >99%.

The logistic regression fitted to the experimental data could discriminate accurately the mortality of *C. flexuosa* from its RWC and PLC (Likelihood ratio test: $\chi^2 = 10.22$, $p < 0.01$; AUC = 0.89; Table 2). The RWC was a stronger predictor of the probability of drought-induced mortality of the evergreen *C. flexuosa* than PLC (Figure 3; Table 2). The *C. flexuosa* odds of mortality increased by 7% for each 1% decrease in RWC ($\chi^2 = 5.58$; $p < 0.02$; Figure 3a). Meanwhile, increasing the PLC by 1% only increased the *C. flexuosa* mortality odds by less than 0.01% ($\chi^2 = 0.0005$; $p = 0.98$; Figure 3b).

Dead *C. flexuosa* individuals had RWC values ranging from 26% to 66%, with a mean of 37.1%, which was significantly lower than the mean RWC of surviving individuals (63.6%; Figure 3c; $t = 4.02$, $p < 0.01$). Meanwhile, the mean PLC in the surviving *C. flexuosa* individuals was 79.98%, which was not statistically different from the mean PLC of 98.56% found in dead individuals (Figure 3d; $t = -1.87$; $p = 0.10$).

3.4 | Leaf area, stomatal conductance and stem diameter responses to drought

The g_s declined similarly in both species during drought (Figure 4; Table S2). The maximum g_s at $P_x = 0$ was similar for both species ($t = -0.004$, $p = 0.99$) as well as the decline rate ($t = -0.64$, $p = 0.53$). The mean g_s of both species at the start of the experiment was

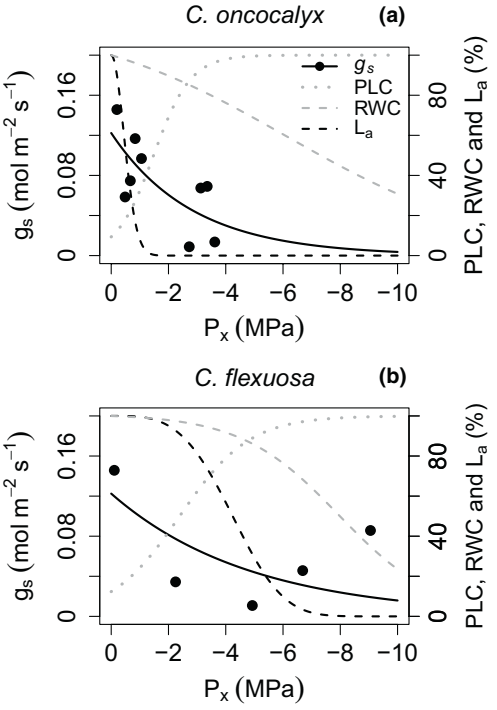


FIGURE 4 Stomatal conductance to water vapour (g_s), total leaf area (L_a) normalised in relation to its maximum value, Relative Water Content in the stem (RWC) and Percentage Loss of xylem hydraulic Conductivity (PLC) as a function of the minimum xylem water pressure (P_x) reached during the drought experiment in the deciduous *Cordia oncocalyx* (a) and the evergreen *Cynophalla flexuosa* (b).

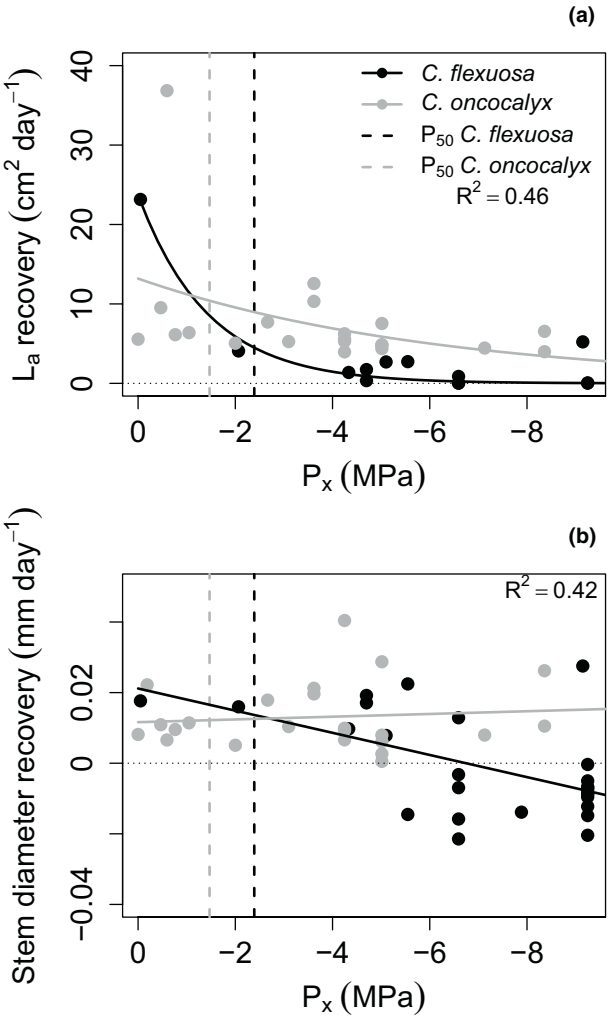


FIGURE 5 Leaf area (a) and stem basal diameter (b) recovery after drought as a function the minimum xylem water pressure (P_x) reached during the drought experiment for the deciduous *Cordia oncocalyx* (grey) and *Cynoplhalla flexuosa* (black). The vertical dashed lines indicate the P_{50} of each species.

approximately 0.12 mol m^{-2} s^{-1} and declined by approximately 20% per MPa increment.

The stomatal closure of both species was only observed at lower RWC and very high PLC (Figure 4). The P_x value that induced 50% stomatal closure ($g_{s,50}$) was close to P_{50} for *C. oncocalyx*, with $g_{s,50}$ equal to −1.97 MPa, while the $g_{s,50}$ for *C. flexuosa* was more negative (−3.39 MPa). The projected 90% stomatal closure was only achieved at −6.55 MPa for *C. oncocalyx* and −11.25 MPa for *C. flexuosa*.

The leaf area of the deciduous *C. oncocalyx* was much more sensitive to P_x than *C. flexuosa* (Figure 4). While *C. oncocalyx* had a higher initial leaf area ($\Delta a = 492.26 \pm 60.82$ cm^2; $t = 7.96$; $p < 0.01$), it declined much faster ($\Delta b = -4.08 \pm 0.25$ MPa; $t = -15.97$; $p < 0.01$). Contrastingly, the stem diameter of the evergreen *C. flexuosa* was more sensitive to P_x than *C. oncocalyx* (Figure S8). The stem diameter of *C. flexuosa* declined 0.19 ± 0.05 mm per MPa ($t = -3.7$, $p < 0.01$), with its growth ceasing completely (i.e. diameter change = 0) at approximately −3.54 MPa. Meanwhile, *C. oncocalyx* had a constant, positive stem diameter changes of 0.95 ± 0.25 cm, regardless of P_x ($\Delta\beta_1 = 0.20 \pm 0.08$, $t = 2.66$, $p = 0.01$; Figure S8).

3.5 | Leaf area and stem diameter recovery after drought

The leaf area and stem diameter recovery of the evergreen *C. flexuosa* were more affected by lower P_x than the deciduous *C. oncocalyx* (Figure 5). The L_a recovery of *C. flexuosa* declined by 50 ± 19% per MPa ($t = -2.67$; $p = 0.01$), while *C. oncocalyx* declined by 14 ± 6% per MPa ($t = -2.42$; $p = 0.02$). The difference in the decline rate (r) between *C. flexuosa* and *C. oncocalyx* was not statistically significant ($\Delta r = 0.35 \pm 0.19$; $t = 1.7$, $p = 0.08$). However, *C. oncocalyx* plants that lost all their leaves during drought have a mean L_a recovery of 5.37 cm^2 day^{-1} afterwards, which was significantly higher than *C. flexuosa* plants that lost all their leaves ($t = -5.80$, $p < 0.01$, Figure S9).

The stem diameter recovery of the evergreen *C. flexuosa* declined by 0.003 ± 0.0009 mm day^{-1} per MPa ($t = -3.57$, $p < 0.01$), which was 0.003 ± 0.001 mm day^{-1} lower than in *C. oncocalyx* ($t = 2.7$, $p = 0.01$; Figure 5b). The linear model fitted to the data predicts that *C. flexuosa* is unable to recover its stem diameter when it reaches a $P_x = -6.82$ MPa, whereas *C. oncocalyx* could recover its stem diameter regardless of the P_x reached during drought.

4 | DISCUSSION

Our findings corroborate the hypothesis that RWC is a better direct predictor of mortality than PLC. Both species could survive even after its xylem was virtually entirely embolised (PLC >99%; Figure 2a). However, the evergreen species started succumbing when its RWC declined below 66% (Figure 3), whereas the deciduous species withstood a PLC >99% for over 20 days and survived even the low RWC reached at the end of the experiment (Figure 2). These contrasting responses support our second hypothesis that deciduous species tolerate desiccation better following hydraulic failure, suggesting that traits such as water storage and leaf shedding are critical predictors of drought mortality, as they regulate post-failure tolerance. Such mechanistic insights are essential for refining models of TSDF responses to climate extremes.

Our experimental design (Figure 1) accurately determined lethal thresholds by monitoring recovery for 3 months post-drought. It linked physiological variables (i.e. PLC and RWC) directly to survival, avoiding biases from apparent or delayed mortality (e.g. Urli et al., 2013). However, a key limitation of our design was our inability to measure P_x, PLC and RWC without interfering with plant recovery. We addressed this limitation by combining a process-based hydraulic model (Supplementary Information S5) with empirical dehydration and vulnerability curves to estimate the PLC and RWC when plants were removed from drought (Figure 1). Our hydraulic model implements the Sperry and Love (2015) theory, previously validated across species and scales (De Cáceres et al., 2022; Sperry et al., 2019; Venturas et al., 2018). The strong agreement between model predictions and dehydration curve results (Figure S7) supports our model application. Additionally, because model predictions based on soil water potential correlated linearly with dehydration curve results based on stem water content, we incorporated soil–root rupture effects (Delval et al., 2025) into our estimates.

4.1 | Critical mortality thresholds

Plant mortality was observed in our experiment only when the stem water content of the evergreen species declined to levels that presumably induced cell membrane destabilisation and subsequent cellular death (see Mantova et al., 2021, 2023). The mean RWC observed in dead *C. flexuosa* plants was 37.13%, which is remarkably similar to the lethal RWC observed in the evergreen *P. menziesii* of 36.9% by Mantova et al. (2021). The deciduous *C. oncocalyx* also reached low RWC (*c.* 35%) at the end of the experiment; however, its RWC was higher than 40% during most of the experiment (Figure 2). The fact that the deciduous species did not die indicates that even low RWC might not be an instantaneous mortality threshold for some species. That is, plants likely die only after dehydration has persisted long enough to cause substantial cell mortality across tissues, rather than immediately after crossing a given RWC threshold. Although *C. oncocalyx* experienced a shorter drought than *C. flexuosa*, the two species were exposed to similar drought intensity. This was probably because *C. oncocalyx* had a greater total leaf area and higher hydraulic conductivity, leading to higher water use rates and faster soil water depletion (Figure 2).

Some of the key traits that might explain the higher tolerance of *C. oncocalyx* to high PLC are its higher total stem water storage and more gradual dehydration curve (Table 1; Figure S5). Although its RWC declined to 50% at a P_x similar to *C. flexuosa*, its SWS was more than twice that of the evergreen species due to this thicker stem, which allows greater water storage. As total plant water storage scales with stem size, it is possible that adult plants in the field would survive even longer after reaching high PLC than the saplings used in our experiment. In addition, *C. oncocalyx's* more gradual dehydration curve means it can retain a higher RWC even at more negative P_x, allowing it to preserve tissue hydration above lethal levels for more time during drought (Figure S5).

Our results indicate that reliable lethal PLC thresholds cannot be established for the studied plants, but we do not claim that these thresholds cannot be established for any other species. Tissue water balance depends on water input from the xylem; consequently, tissue desiccation is, at least partly, caused by hydraulic failure. However, our results (Figure 2) and other studies (Mantova et al., 2021, 2023) show a delay between hydraulic failure and tissue dehydration and subsequent mortality. This delay might be the consequence of different traits, such as residual water losses, tissue total water content and hydraulic capacitance (see Blackman et al., 2016), influencing the time it takes for the plant cells to reach their lethal RWC after hydraulic failure. Depending on these traits, the delay between hydraulic failure and tissue desiccation may be negligible, so PLC thresholds could still be an effective predictor of mortality in these cases (e.g. Brodribb & Cochard, 2009; Hammond et al., 2019; Urli et al., 2013).

Plants from arid and semiarid environments, such as Caatinga, could benefit from traits that preserve tissue hydration even after hydraulic failure, resulting in a large delay between xylem dysfunction and tissue dehydration and mortality (Figure 2). Caatinga plants often grow in shallow soils with low water storage capacity (Pinheiro et al., 2013) and are exposed annually to a long dry season with very low precipitation and high atmospheric evaporative demand (Mutti et al., 2019; Sampaio, 1995). In these circumstances, the xylem water pressure in many Caatinga plants is negative enough during the dry season to induce high levels of embolism regardless of stomatal regulation, leaf phenology or xylem resistance to embolism (Lima et al., 2018; Souza et al., 2020). Consequently, plant survival in Caatinga might depend on functional traits to maintain tissue hydration after hydraulic failure. This would explain why functional strategies such as water storage and leaf shedding to minimise residual water loss are common in Caatinga (Lima et al., 2012; Wright et al., 2021). Evergreen Caatinga plants that do not exhibit these strategies, such as *C. flexuosa*, typically occur in less arid sites and regions with deeper soils where these species can produce deeper root systems (Lopes et al., 2022; Oliveira et al., 2024).

4.2 | Responses to drought and recovery after drought

Both species would sustain leaf gas exchange even at high PLC levels (Figure 4), which implies short-term carbon gain is favoured over embolism avoidance in these species. Many species close their stomata before the onset of xylem embolism (Creek et al., 2020). However, theoretical models suggest that sacrificing a fraction of the xylem hydraulic conductance to sustain carbon assimilation might be the optimal stomatal regulation strategy under certain circumstances (Eller et al., 2018, 2020; Jones & Sutherland, 1991; Potkay & Feng, 2023). This type of acquisitive stomatal regulation has also been observed in other species (Franks et al., 2007; Peters et al., 2023; Pivovaroff et al., 2018). This stomatal regulation strategy might allow evergreen species to maximise carbon uptake during the dry season and compensate for their higher carbon investment in tissue construction (Poorter et al., 2009; Ribeiro et al., 2022; Souza et al., 2020). However, this strategy might pose increased risks for evergreen species' survival in sites exposed to more intense droughts and contribute to their more restricted distribution (Oliveira et al., 2024).

The deciduous species relied on leaf shedding to act as hydraulic fuses and minimise water loss during drought and delay both hydraulic failure and desiccation (Figure 4). The deciduous species could quickly recover its leaf area and stem growth after drought (Figure 5), which suggests that this species might rely on stored carbon reserves to sustain tissue production post-drought (Piper & Fajardo, 2014; Pratt et al., 2021). Meanwhile, the evergreen species exhibited a strong drought legacy effect when it was exposed to more severe drought (Figure 5; Figure S8). It is possible that the evergreen species did not have enough stored carbon to sustain the production of large volumes of its more costly tissues (Souza et al., 2020). Consequently, it had to rely on carbon assimilation from a reduced crown and immature leaves to sustain its recovery.

5 | CONCLUSIONS

Our results challenge the prevailing assumption that critical PLC thresholds universally trigger mortality, highlighting instead the role of RWC as a useful predictor of plant mortality under drought. Our findings show that hydraulic failure alone is not equally lethal to all plants during drought. However, our findings should not be interpreted as if hydraulic failure is not important to drought-induced mortality, only that processes that occur after hydraulic failure and are governed by a different suite of functional traits are also relevant. The RWC thresholds we found for the evergreen species can be used to extend current plant hydraulic models (De Cáceres et al., 2022; Eller et al., 2018, 2020; Venturas et al., 2021) and allow them to also predict relevant demographic processes, such as drought-induced mortality rates. In addition, these lethal RWC thresholds could be used to monitor large-scale vegetation mortality risks if combined with remote sensing methods to assess vegetation water content (Konings et al., 2019).

We also show that evergreen TSDF species succumb faster during drought than deciduous species, which can withstand longer periods after their xylem collapses and quickly recover afterwards. These findings can help to explain the differences in distribution of evergreen and deciduous TSDF species (Oliveira et al., 2024) and their differential responses to climate change (Carvalho et al., 2023).

AUTHOR CONTRIBUTIONS

Cleiton Breder Eller and Lussarina Oliveira Lima conceived the research and designed the experiment; Lussarina Oliveira Lima, Angela Lucena Nascimento Jesus and Vivian Barros Talmag collected the data; Cleiton Breder Eller and Lussarina Oliveira Lima analysed the data; Cleiton Breder Eller, Lussarina Oliveira Lima, Rafael Silva Oliveira, Francisca Soares de Araújo and Arlete Aparecida Soares led the writing of the manuscript. All authors contributed critically to the drafts and gave final approval for publication.

ACKNOWLEDGEMENTS

We thank Diogo Menezes for contributing to the data collection. This research was conducted under the National Institute of Science and Technology for Interdisciplinary and Transdisciplinary Studies in Ecology and Evolution (INCT INTREE) and was funded by the National Council for Scientific and Technological Development (CNPq) - Brazil (Grant: 408930/2024-1) and, in part, by the São Paulo Research Foundation (FAPESP) - Brazil (Process Number #2025/28192-8). This study was also financed by the Coordenação de Aperfeiçoamento de Pessoal de Nível Superior—Brasil (CAPES)—Finance Code 001 and by the grant AJC-0222-00006.01.00/24 awarded to C.B.E. by the Serrapilheira Institute and the Fundação Cearense de Apoio ao Desenvolvimento Científico e Tecnológico (FUNCAP), and the scholarship awarded to L.O.L. by FUNCAP. R.S.O., A.A.S and F.S.A. acknowledge the Conselho Nacional de Desenvolvimento Científico e Tecnológico (CNPq) for Research Productivity Fellowships.

CONFLICT OF INTEREST STATEMENT

The authors declare no conflicts of interest.

DATA AVAILABILITY STATEMENT

The data that support the findings of this study are available in Zenodo at https://doi.org/10.5281/zenodo.21727546 (Lima et al., 2026).

ORCID

Lussarina Oliveira Lima https://orcid.org/0009-0004-1459-2737
Angela Lucena Nascimento Jesus https://orcid.org/0000-0003-0101-0924
Rafael Silva Oliveira https://orcid.org/0000-0002-6392-2526
Francisca Soares de Araújo https://orcid.org/0000-0003-4661-6137
Arlete Aparecida Soares https://orcid.org/0000-0002-0329-0619
Cleiton Breder Eller https://orcid.org/0000-0002-7795-2574

REFERENCES

Accioly, A. N., de Paiva Farias, R., & de Arruda, E. C. P. (2024). Plants in the caatinga possess multiple adaptative leaf morphoanatomical traits concurrently, a pattern revealed from a systematic review. *Journal of Arid Environments*, *222*, 105162.

Adams, H. D., Zeppel, M. J., Anderegg, W. R., Hartmann, H., Landhäusser, S. M., Tissue, D. T., Huxman, T. E., Hudson, P. J., Franz, T. E., Allen, C. D., Anderegg, L. D. L., Barron-Gafford, G. A., Beerling, D. J., Breshears, D. D., Brodribb, T. J., Bugmann, H., Cobb, R. C., Collins, A. D., Dickman, L. T., … McDowell, N. G. (2017). A multi-species synthesis of physiological mechanisms in drought-induced tree mortality. *Nature Ecology & Evolution*, *1*(9), 1285–1291.

Allen, C. D., Macalady, A. K., Chenchouni, H., Bachelet, D., McDowell, N., Vennetier, M., Kitzberger, T., Rigling, A., Breshears, D. D., Hogg, E. H. (Ted), Gonzalez, P., Fensham, R., Zhang, Z., Castro, J., Demidova, N., Lim, J.-H., Allard, G., Running, S. W., Semerci, A., … Cobb, N. (2010). A global overview of drought and heat-induced tree mortality reveals emerging climate change risks for forests. *Forest Ecology and Management*, *259*(4), 660–684.

Araújo, K. C., Souza, B. C., Carvalho, E. C. D., Freire, R. S., Teixeira, A. S., Muniz, C. R., Martins, F. R., Oliveira, R. S., Eller, C. B., & Soares, A. A. (2024). The multiple roles of trichomes in two croton species. *Plant, Cell & Environment*, *47*(5), 1685–1700.

Blackman, C. J., Pfautsch, S., Choat, B., Delzon, S., Gleason, S. M., & Duursma, R. A. (2016). Toward an index of desiccation time to tree mortality under drought. *Plant, Cell & Environment*, *39*(10), 2342–2345.

Breusch, T. S., & Pagan, A. R. (1979). A simple test for heteroscedasticity and random coefficient variation. *Econometrica: Journal of the Econometric Society*, *47*, 1287–1294.

Brodribb, T. J., & Cochard, H. (2009). Hydraulic failure defines the recovery and point of death in water-stressed conifers. *Plant Physiology*, *149*, 575–584.

Carvalho, C. E., Sfair, J. C., Eller, C. B., Menezes, B. S., Menezes, M. O., & Araújo, F. S. (2023). Tree height, leaf thickness and seed size drive Caatinga plants' sensitivity to climate change. *Journal of Biogeography*, *50*(12), 2057–2068.

Choat, B., Brodribb, T. J., Brodersen, C. R., Duursma, R. A., López, R., & Medlyn, B. E. (2018). Triggers of tree mortality under drought. *Nature*, *558*(7711), 531–539.

Choat, B., Nolf, M., Lopez, R., Peters, J. M., Carins-Murphy, M. R., Creek, D., & Brodribb, T. J. (2019). Non-invasive imaging shows no evidence of embolism repair after drought in tree species of two genera. *Tree Physiology*, *39*(1), 113–121.

Creek, D., Lamarque, L. J., Torres-Ruiz, J. M., Parise, C., Burlett, R., Tissue, D. T., & Delzon, S. (2020). Xylem embolism in leaves does not occur with open stomata: Evidence from direct observations using the optical visualization technique. *Journal of Experimental Botany*, *71*(3), 1151–1159.

De Cáceres, M., Molowny-Horas, R., Cabon, A., Martínez-Vilalta, J., Mencuccini, M., García-Valdés, R., Nadal-Sala, D., Sabaté, S., Martin-StPaul, N., Morin, X., D'Adamo, F., Batllori, E., & Améztegui, A. (2022). MEDFATE 2.8. 1: A trait-enabled model to simulate Mediterranean forest function and dynamics at regional scales. *Geoscientific Model Development Discussions*, *2022*, 1–52.

Delval, L., Vanderborght, J., & Javaux, M. (2025). Combination of plant and soil water potential monitoring and modelling demonstrates soil-root hydraulic disconnection during drought. *Plant and Soil*, *511*(1), 1449–1472.

Eller, C. B., Rowland, L., Mencuccini, M., Rosas, T., Williams, K., Harper, A., Medlyn, B. E., Wagner, Y., Klein, T., Teodoro, G. S., Oliveira, R. S., Matos, I. S., Rosado, B. H. P., Fuchs, K., Wohlfahrt, G., Montagnani, L., Meir, P., Sitch, S., & Cox, P. M. (2020). Stomatal optimization based on xylem hydraulics (SOX) improves land surface model simulation of vegetation responses to climate. *New Phytologist*, *226*(6), 1622–1637.

Eller, C. B., Rowland, L., Oliveira, R. S., Bittencourt, P. R., Barros, F. V., Da Costa, A. C., Meir, P., Friend, A. D., Mencuccini, M., Sitch, S., & Cox, P. (2018). Modelling tropical forest responses to drought and El Niño with a stomatal optimization model based on xylem hydraulics. *Philosophical Transactions of the Royal Society, B: Biological Sciences*, *373*(1760), 20170315.

Franks, P. J., Drake, P. L., & Froend, R. H. (2007). Anisohydric but isohydrodynamic: Seasonally constant plant water potential gradient explained by a stomatal control mechanism incorporating variable plant hydraulic conductance. *Plant, Cell & Environment*, *30*(1), 19–30.

Hammond, W. M., Williams, A. P., Abatzoglou, J. T., Adams, H. D., Klein, T., López, R., Sáenz-Romero, C., Hartmann, H., Breshears, D. D., & Allen, C. D. (2022). Global field observations of tree die-off reveal hotter-drought fingerprint for Earth's forests. *Nature Communications*, *13*(1), 1761.

Hammond, W. M., Yu, K., Wilson, L. A., Will, R. E., Anderegg, W. R., & Adams, H. D. (2019). Dead or dying? Quantifying the point of no return from hydraulic failure in drought-induced tree mortality. *New Phytologist*, *223*(4), 1834–1843.

Heinze, G., & Schemper, M. (2002). A solution to the problem of separation in logistic regression. *Statistics in Medicine*, *21*, 2409–2419.

Holanda, A. E. R., Souza, B. C., Carvalho, E. C. D., Oliveira, R. S., Martins, F. R., Muniz, C. R., Costa, R. C., & Soares, A. A. (2019). How do leaf wetting events affect gas exchange and leaf lifespan of plants from seasonally dry tropical vegetation? *Plant Biology*, *21*(6), 1097–1109.

Hosmer, D. W., Jr., Lemeshow, S., & Sturdivant, R. X. (2013). *Applied logistic regression*. John Wiley & Sons.

Jones, H. G., & Sutherland, R. A. (1991). Stomatal control of xylem embolism. *Plant, Cell & Environment*, *14*, 607–612.

Koenker, R. (1981). A note on studentizing a test for heteroscedasticity. *Journal of Econometrics*, *17*(1), 107–112.

Konings, A. G., Rao, K., & Steele-Dunne, S. C. (2019). Macro to micro: Microwave remote sensing of plant water content for physiology and ecology. *New Phytologist*, *223*(3), 1166–1172.

Kursar, T. A., Engelbrecht, B. M., Burke, A., Tyree, M. T., El Omari, B., & Giraldo, J. P. (2009). Tolerance to low leaf water status of tropical tree seedlings is related to drought performance and distribution. *Functional Ecology*, *23*(1), 93–102.

Lima, A. L. A., de Sá Barretto Sampaio, E. V., de Castro, C. C., Rodal, M. J. N., Antonino, A. C. D., & de Melo, A. L. (2012). Do the phenology and functional stem attributes of woody species allow for the identification of functional groups in the semiarid region of Brazil? *Trees*, *26*(5), 1605–1616.

Lima, L. O., Jesus, A. L. N., Talmag, V. B., Oliveira, R. S., Araújo, F. S., Soares, A. A., & Eller, C. B. (2026). Data for: Stem water content predicts drought-induced mortality in tropical semiarid species [dataset]. *Zenodo*. https://doi.org/10.5281/zenodo.21727546

Lima, T. R., Carvalho, E. C., Martins, F. R., Oliveira, R. S., Miranda, R. S., Müller, C. S., Pereira, L., Bittencourt, P. R. L., Sobczak, J. C. M. S. M., Gomes-Filho, E., Costa, R. C., & Araújo, F. S. (2018). Lignin composition is related to xylem embolism resistance and leaf life span in trees in a tropical semiarid climate. *New Phytologist*, *219*(4), 1252–1262.

Lopes, R. F., Melo, A. S., & Santos, M. G. (2022). Drought tolerance mechanisms of a woody evergreen in a tropical dry forest. *Theoretical and Experimental Plant Physiology*, *34*(3), 433–445.

Love, D. M., & Sperry, J. S. (2018). In situ embolism induction reveals vessel refilling in a natural aspen stand. *Tree Physiology*, *38*(7), 1006–1015.

Maass, J. M., Balvanera, P., Castillo, A., Daily, G. C., Mooney, H. A., Ehrlich, P., Quesada, M., Miranda, A., Jaramillo, V. J., García-Oliva, F., Martínez-Yrizar, A., Cotler, H., López-Blanco, J., Pérez-Jiménez, A., Búrquez, A., Tinoco, C., Ceballos, G., Barraza, L., Ayala, R., & Sarukhán, J. (2005). Ecosystem services of tropical dry forests: Insights from long-term ecological and social research on the Pacific Coast of Mexico. *Ecology and Society*, *10*(1), 23.

Mantova, M., Cochard, H., Burlett, R., Delzon, S., King, A., Rodriguez-Dominguez, C. M., Ahmed, M. A., Trueba, S., & Torres-Ruiz, J. M. (2023). On the path from xylem hydraulic failure to downstream cell death. *New Phytologist*, *237*(3), 793–806.

Mantova, M., Menezes-Silva, P. E., Badel, E., Cochard, H., & Torres-Ruiz, J. M. (2021). The interplay of hydraulic failure and cell vitality explains tree capacity to recover from drought. *Physiologia Plantarum*, *172*(1), 247–257.

Marengo, J. A., Torres, R. R., & Alves, L. M. (2017). Drought in Northeast Brazil—Past, present, and future. *Theoretical and Applied Climatology*, *129*, 1189–1200.

Martinez-Vilalta, J., Anderegg, W. R., Sapes, G., & Sala, A. (2019). Greater focus on water pools may improve our ability to understand and anticipate drought-induced mortality in plants. *New Phytologist*, *223*(1), 22–32.

McDowell, N., Pockman, W. T., Allen, C. D., Breshears, D. D., Cobb, N., Kolb, T., Kolb, T., Plaut, J., Sperry, J., West, A., Williams, D. G., & Yepez, E. A. (2008). Mechanisms of plant survival and mortality during drought: Why do some plants survive while others succumb to drought? *New Phytologist*, *178*(4), 719–739.

McDowell, N. G., Fisher, R. A., Xu, C., Domec, J. C., Hölttä, T., Mackay, D. S., Sperry, J. S., Boutz, A., Dickman, L., Gehres, N., Limousin, J. M., Macalady, A., Martínez-Vilalta, J., Mencuccini, M., Plaut, J. A., Ogée, J., Pangle, R. E., Rasse, D. P., Ryan, M. G., … Pockman, W. T. (2013). Evaluating theories of drought-induced vegetation mortality using a multimodel–experiment framework. *New Phytologist*, *200*(2), 304–321.

McDowell, N. G., Sapes, G., Pivovaroff, A., Adams, H. D., Allen, C. D., Anderegg, W. R., Arend, M., Breshears, D. D., Brodribb, T., Choat, B., Cochard, H., De Cáceres, M., De Kauwe, M. G., Grossiord, C., Hammond, W. M., Hartmann, H., Hoch, G., Kahmen, A., Klein, T., … Xu, C. (2022). Mechanisms of woody-plant mortality under rising drought, CO_2 and vapour pressure deficit. *Nature Reviews Earth & Environment*, *3*(5), 294–308.

Moro, M. F., Lughadha, E. N., De Araújo, F. S., & Martins, F. R. (2016). A phytogeographical metaanalysis of the semiarid Caatinga domain in Brazil. *The Botanical Review*, *82*, 91–148.

Muenchow, J., Dieker, P., Kluge, J., Kessler, M., & von Wehrden, H. (2018). A review of ecological gradient research in the tropics: Identifying research gaps, future directions, and conservation priorities. *Biodiversity and Conservation*, *27*(2), 273–285.

Murphy, P. G., & Lugo, A. E. (1986). Ecology of tropical dry forest. *Annual Review of Ecology and Systematics*, *17*, 67–88.

Mutti, P. R., da Silva, L. L., Medeiros, S. D. S., Dubreuil, V., Mendes, K. R., Marques, T. V., Lúcio, P. S., Silva, C. M. S. e., & Bezerra, B. G. (2019). Basin scale rainfall-evapotranspiration dynamics in a tropical semi-arid environment during dry and wet years. *International Journal of Applied Earth Observation and Geoinformation*, *75*, 29–43.

Nardini, A., Gullo, M. A. L., & Salleo, S. (2011). Refilling embolized xylem conduits: Is it a matter of phloem unloading? *Plant Science*, *180*(4), 604–611.

Oliveira, A. C., Nunes, A., Oliveira, M. A., Oliveira, R. S., Rodrigues, R. G., & Branquinho, C. (2024). Shifts in plant functional groups along an aridity gradient in a tropical dry forest. *Science of the Total Environment*, *989*, 171695.

Oliveira, R. S., Eller, C. B., Barros, F. D., Hirota, M., Brum, M., & Bittencourt, P. (2021). Linking plant hydraulics and the fast–slow continuum to understand resilience to drought in tropical ecosystems. *New Phytologist*, *230*(3), 904–923.

Pammenter, N. W., & Van Der Willigen, C. (1998). A mathematical and statistical analysis of the curves illustrating vulnerability of xylem to cavitation. *Tree Physiology*, *18*, 589–593.

Pereira, S., Figueiredo-Lima, K., Oliveira, A. F. M., & Santos, M. G. (2019). Changes in foliar epicuticular wax and photosynthesis metabolism in evergreen woody species under different soil water availability. *Photosynthetica*, *57*(1), 192–201.

Peters, R. L., Steppe, K., Pappas, C., Zweifel, R., Babst, F., Dietrich, L., von Arx, G., Poyatos, R., Fonti, M., Fonti, P., Grossiord, C., Gharun, M., Buchmann, N., Steger, D. N., & Kahmen, A. (2023). Daytime stomatal regulation in mature temperate trees prioritizes stem rehydration at night. *New Phytologist*, *239*(2), 533–546.

Pinheiro, E. A. R., Costa, C. A. G., & De Araújo, J. C. (2013). Effective root depth of the Caatinga biome. *Journal of Arid Environments*, *89*, 1–4.

Piper, F. I., & Fajardo, A. (2014). Foliar habit, tolerance to defoliation and their link to carbon and nitrogen storage. *Journal of Ecology*, *102*, 1101–1111.

Pivovaroff, A. L., Cook, V. M., & Santiago, L. S. (2018). Stomatal behaviour and stem xylem traits are coordinated for woody plant species under exceptional drought conditions. *Plant, Cell & Environment*, *41*(11), 2617–2626.

Poorter, H., Niinemets, Ü., Poorter, L., Wright, I. J., & Villar, R. (2009). Causes and consequences of variation in leaf mass per area (LMA): A meta-analysis. *New Phytologist*, *182*, 565–588.

Potkay, A., & Feng, X. (2023). Do stomata optimize turgor-driven growth? A new framework for integrating stomata response with whole-plant hydraulics and carbon balance. *New Phytologist*, *238*(2), 506–528.

Pratt, R. B., Tobin, M. F., Jacobsen, A. L., Traugh, C. A., De Guzman, M. E., Hayes, C. C., Toschi, H. S., MacKinnon, E. D., Percolla, M. I., Clem, M. E., & Smith, P. T. (2021). Starch storage capacity of sapwood is related to dehydration avoidance during drought. *American Journal of Botany*, *108*(1), 91–101.

R Core Team. (2024). *R: A language and environment for statistical computing*. R Foundation for Statistical Computing. https://www.R-project.org/

Ribeiro, D. R., Silva, J. L. A., Do Nascimento, M. T., & Vitória, A. P. (2022). Leaf habits and their relationship with leaf and wood traits in tropical dry forests. *Trees*, *36*, 7–24.

Sampaio, E. S. B. (1995). Overview of the Brazilian caatinga. In S. H. Bullock, H. A.Mooney, & E.Medina (Eds.), *Seasonally dry tropical forests* (pp. 35–63). Cambridge University Press.

Siyum, Z. G. (2020). Tropical dry forest dynamics in the context of climate change: Syntheses of drivers, gaps, and management perspectives. *Ecological Processes*, *9*(1), 1–16.

Souza, B. C., Carvalho, E. C. D., Oliveira, R. S., de Araujo, F. S., de Lima, A. L. A., & Rodal, M. J. N. (2020). Drought response strategies of deciduous and evergreen woody species in a seasonally dry neotropical forest. *Oecologia*, *194*(1), 221–236.

Sperry, J. S., Donnelly, J. R., & Tyree, M. T. (1988). A method for measuring hydraulic conductivity and embolism in xylem. *Plant, Cell & Environment*, *11*, 35–40.

Sperry, J. S., & Love, D. M. (2015). What plant hydraulics can tell us about responses to climate-change droughts. *New Phytologist*, *207*, 14–27.

Sperry, J. S., Venturas, M. D., Todd, H. N., Trugman, A. T., Anderegg, W. R., Wang, Y., & Tai, X. (2019). The impact of rising CO_2 and acclimation on the response of US forests to global warming. *Proceedings of the National Academy of Sciences of the United States of America*, *116*(51), 25734–25744.

Tomasella, J., Do Amaral Cunha, A. M., Zeri, M., & Costa, L. C. (2025). Changes in the aridity index across Brazilian biomes. *Science of the Total Environment*, *989*, 179869.

Tomlinson, K. W., Poorter, L., Sterck, F. J., Borghetti, F., Ward, D., de Bie, S., & van Langevelde, F. (2013). Leaf adaptations of evergreen and deciduous trees of semi-arid and humid savannas on three continents. *Journal of Ecology*, *101*(2), 430–440.

Trugman, A. T., Anderegg, L. D., Anderegg, W. R., Das, A. J., & Stephenson, N. L. (2021). Why is tree drought mortality so hard to predict? *Trends in Ecology & Evolution*, *36*(6), 520–532.

Tyree, M. T., Engelbrecht, B. M., Vargas, G., & Kursar, T. A. (2003). Desiccation tolerance of five tropical seedlings in Panama. Relationship to a field assessment of drought performance. *Plant Physiology*, *132*(3), 1439–1447.

Urli, M., Porté, A. J., Cochard, H., Guengant, Y., Burlett, R., & Delzon, S. (2013). Xylem embolism threshold for catastrophic hydraulic failure in angiosperm trees. *Tree Physiology*, *33*(7), 672–683.

Van Genuchten, M. T. (1980). A closed-form equation for predicting the hydraulic conductivity of unsaturated soils. *Soil Science Society of America Journal*, *44*, 892–898.

Venturas, M. D., Sperry, J. S., Love, D. M., Frehner, E. H., Allred, M. G., Wang, Y., & Anderegg, W. R. (2018). A stomatal control model based on optimization of carbon gain versus hydraulic risk predicts aspen sapling responses to drought. *New Phytologist*, *220*(3), 836–850.

Venturas, M. D., Todd, H. N., Trugman, A. T., & Anderegg, W. R. (2021). Understanding and predicting forest mortality in the western United States using long-term forest inventory data and modeled hydraulic damage. *New Phytologist*, *230*(5), 1896–1910.

Wright, C. L., de Lima, A. L., de Souza, E. S., West, J. B., & Wilcox, B. P. (2021). Plant functional types broadly describe water use strategies in the Caatinga, a seasonally dry tropical forest in northeast Brazil. *Ecology and Evolution*, *11*(17), 11808–11825.

Zuur, A. F., Ieno, E. N., & Elphick, C. S. (2010). A protocol for data exploration to avoid common statistical problems. *Methods in Ecology and Evolution*, *1*(1), 3–14.

SUPPORTING INFORMATION

Additional supporting information can be found online in the Supporting Information section at the end of this article.

Supporting Information S1. Leaf area calculations.

Supporting Information S2. Calibration of soil water content.

Supporting Information S3. Soil water potential calculation.

Supporting Information S4. Xylem vulnerability to embolism.

Supporting Information S5. Modelling xylem water pressure.

Figure S1. Environment data during the experiments of drought with species Cordia oncocalyx and Cynophalla flexuosa.

Figure S2. Relationship between soil water content (θ) measured gravimetrically and volumetric soil water content (VWC) measured with a portable sensor (Hydrosense II, Campbell Sensor, USA).

Figure S3. Observed soil water potential (P_s) and water content (θ) measured in drying soils (points) and the predictions from the Van Genuchten model fitted to this data (line).

Figure S4. Seedlings of the species Cordia oncocalyx (a) and Cynophalla flexuosa (b) at the start of the drought experiment.

Figure S5. Relationship between Relative Water Content in the stem (RWC) and the xylem water pressure (P_x) for Cordia oncocalyx (a) and Cynophalla flexuosa (b).

Figure S6. Vulnerability curves to embolism for the deciduous species Cordia oncocalyx (a) and evergreen Cynophalla flexuosa (b).

Figure S7. Relationship between xylem water pressure (P_x) estimated from the P_x curve and relative water content in the stem (RWC; Equation 5; *y*-axis) and soil water potential (P_s) estimated from soil water content data (θ) using the Van Genuchten model (1980) (Equation S5; *x*-axis).

Figure S8. Stem basal diameter changes as a function of the minimum xylem water pressure (P_x) reached during the drought experiment in the deciduous Cordia oncocalyx (grey) and the evergreen Cynophalla flexuosa (black). The vertical dashed lines indicate the P50 of each species.

Figure S9. Boxplot of the La recovery in leafless plants of Cordia oncocalyx and Cynophalla flexuosa after the drought experiment.

Table S1. Fitted Van Genuchten (1980) model parameters.

Table S2. Estimated parameters of the nonlinear model (Equation 12) fitted to the effect of xylem water potential (P_x) on stomatal conductance (g_s) in species *Cordia oncocalyx* and *Cynophalla flexuosa*.

How to cite this article: Lima, L. O., Lucena Nascimento Jesus, A., Talmag, V. B., Oliveira, R. S., Soares de Araújo, F., Soares, A. A., & Eller, C. B. (2026). Stem water content predicts drought-induced mortality in tropical semiarid species. *Functional Ecology*, *40*, 3318–3331. https://doi.org/10.1111/1365-2435.70439